ISSN: 0128-7680
Pertanika J. Sci. & Technol. **17 (2)**: 269 – 289 (2009)

Study of CNG Combustion Under Internal Combustion Engines Conditions Part I: Using Quasi-Dimensional Modelling

Y. Bakhshan[1*] and Shahrir Abdullah[2]
[1]Department of Mechanical Engineering,
University of Hormozgan,
P.O.Box 3995,
[2]Department of Mechanical and Material Engineering,
Universiti Kebangsaan Malaysia,
43600 UKM Bangi, Selangor, Malaysia
[*]E-mail: y_bakhshan@yahoo.com

ABSTRACT

An in-house quasi-dimensional code has been developed which simulate the overlap, intake, compression, combustion, as well as expansion and exhaust processes of a homogeneous charged internal combustion engine (ICE). A detailed chemical kinetic mechanism, constituting of 39 species and 148 elementary reactions, has been used in conjunction with above code to study the combustion of CNG under IC engine conditions. Two different criteria, based on pressure rise and mass of fuel burned, are used to detect the onset of ignition. Parametric studies are conducted to show the effect of compression ratio, initial pressure, intake temperature and equivalence ratio, on the time of ignition and fuel burning rate. The results obtained from the modelling show a good agreement with the experimental data.

Keywords: Natural gas, auto-ignition, quasi-dimensional, chemical kinetic, modelling

NOTATION

θ	Crank angle (Deg.)
φ	Equivalence ratio
C_v, C_p	Specific heat capacity (Kj/Kg.K)
A_v	Area (m^2)
h	Enthalpy (Kj/Kg)
h_f	Enthalpy of formation (Kj/Kg)
A	Air (Kg)
B	Cylinder bore (m)
F	Fuel (kg)
W	Molecular weight (Kg)
m	Mass (Kg)
$\dot{m}_i$	Mass flows rate into the cylinder (Kg/s)
$\dot{m}_e$	Mass flows rate out of the cylinder (Kg/s)
ρ	Density (Kg/m^3)
V	Volume (m^3)

Received: 3 March 2008
Accepted: 25 February 2009
[*]Corresponding Author

t Time (s)
T Temperature (K)
$E_{fn,rn}$ Activation energy (J/mol)
$\beta_{fn,rn}$ Reaction constant
K_{fn},K_{rn} Reaction rate Constants

SUBSCRIPTS AND SUPERSCRIPTS

g Gas
fn Forward
rn Backward

ABBREVIATIONS

NOx Oxides of nitrogen
TDC Top dead center
ATDC After top dead center
BBDC Before bottom dead center
BTDC Before top dead center
ABDC After bottom dead center
ICE Internal combustion engine
CNG Compressed natural gas

INTRODUCTION

Natural gas is an economical and clean burning fuel, whose advantages as an alternative fuel for internal combustion engines have been well documented (Papageorgakis, 1997; Emad Boshra Fawzy Khalil, 2000; Bade Shrestha, 1999). Experiments in a combustion bomb have shown that auto-ignition of natural gas, under diesel-like conditions, requires a temperature as high as 1100-1200K (Papageorgakis, 1997). This high temperature requirement mandates that either a high compression ratio (about 23:1) or a high intake air temperature be used, both of which have negative effects on the performance and durability of engine. Obviously, knowing at what conditions of temperatures, pressures, and compositions, a methane-air mixture can have auto-ignition, or whether ignition assists in the form of glow plug, is very important. A fundamental understanding of the thermodynamics and fuel composition-related factors influencing ignition in internal combustion engines can only be obtained from a detailed study of the processes leading up to auto-ignition. However, the inherent transient nature of this starting process, with reactants and evolving towards a steadily burning flame, makes its theoretical treatment difficult. Recourse must almost always be made the numerical techniques involving the solution time-dependent equations of mass, momentum and energy which include the effect of chemical reactions and account for molecular transport, thermodynamics and convection. The usual approach used in studying the problem of ignition has either been to ignore the details of chemistry or to ignore the details of flow, the overriding concern being the enormous computational costs involved in combining the two, while the importance of detailed chemistry in homogeneous studies of ignition and flame propagation is well-documented (Emad Boshra Fawzy Khalil, 2000). Sloane and Ronny (Zhou, 1993) showed that although properly-calibrated one-step models are able to describe flame speed for planar flame propagation reasonably well, they are very inadequate in accurately predicting the minimum ignition energy and induction time. In fact, the induction time for homogeneous ignition of methane-air mixture, predicted using the one-step models, was about 60 to 1500 times lower than the one predicted using a detailed kinetic mechanism over a range of temperatures (1500 to 2222 K) (Zhou, 1993).

The objectives of this work were to explain the predictive ability of the coupled model in simulating the auto- ignition of natural gas injected in an ICE, and to study the effect of important parameters on the ignition of a CNG engine.

GOVERNING EQUATIONS

Quasi-Dimensional Engine Simulation

This simulation starts with a thermodynamic-based in-cylinder model. The structure of this type of engine simulation is as follows. The model divides the complete cycle into overlap, intake, compression, combustion, expansion and exhaust processes. Some of the applied equations in this simulation are as follow:
Work is defined by:

$$\dot{W} = P\dot{V} \tag{1}$$

and specific enthalpy by

$$\dot{h} = C_P\dot{T} + \frac{\partial h}{\partial P}\dot{P} + \frac{\partial h}{\partial \varphi}\dot{\varphi} \tag{2}$$

State equation:

$$\begin{aligned} &PV = MR_gT \\ &\frac{\dot{P}}{P} + \frac{\dot{V}}{V} = \frac{\dot{M}}{M} + \frac{\dot{T}}{T} \\ &R_g = R_g(T,P,\varphi) \end{aligned} \tag{3}$$

Energy equation for an open system:

$$\dot{E} = \dot{Q} - \dot{W} + \dot{M}_{in}h_{in} - \dot{M}_{out}h_{out} \tag{4}$$

The volume constraint is given by:

$$\dot{V} = \sum_{i=1}^{n} \dot{V}_i \tag{5}$$

and the equivalence ratio is:

$$\dot{\varphi}_i = \frac{\varphi_i(t+\Delta t) - \varphi(t)}{\Delta t} \tag{6}$$

and,

$$\varphi_i(t+\Delta t) = \frac{F_i / A_i}{(F/A)_s} \tag{7}$$

Where, F_i and A_i are the quantity of fuel and air, respectively.

Gas Exchange Model

A one-dimensional quasi-steady compressible flow model is used to describe the gas exchange between the engine cylinder and intake and exhaust manifolds.

The governing equations can be written as follows:

$$\dot{m} = C_v A_v \left(\frac{RT_o}{P_o}\right)\left(\gamma RT_o\right)^{1/2} * \left\{\left(\frac{2}{\gamma-1}\right)\left[\left(\frac{P_2}{P_o}\right)^{2/\gamma} - \left(\frac{P_2}{P_o}\right)^{\frac{\gamma+1}{2}}\right\}^{\frac{1}{2}} \quad (8)$$

For choked flow

$$\dot{m} = C_v A_v \left(\frac{RT_{oc}}{P_{oc}}\right)\left(\gamma RT_o\right)^{1/2} * \left\{\left(\frac{2}{\gamma+1}\right)^{\frac{\gamma+1}{\gamma-1}}\right\}^{\frac{1}{2}} \quad (9)$$

More details about the quasi-dimensional modeling can be found in other papers by authors in references (Mansouri and Bakhshan, 2000; Mansouri and Bakhshan, 2001; Mansouri and Heywood, 1980; Mansouri and Bakhshan, 2000; Bakhshan, Karim and Mansouri, 2002; Bakhshan, Karim and Mansouri, 2003).

Chemical Kinetic Modelling

There has been a significant and progress made in recent years in the status of chemical kinetic modelling of the combustion of hydrocarbon fuels under engine-like conditions. These enable the derivation of comprehensive chemical kinetic models for hydrocarbons. Such schemes can be incorporated into a variety of predictive models so as to analyse the performance of engine under operating and design conditions, with a reasonable level of confidence. They may also be used to validate the results of other models which employ only reduced kinetic schemes for a wide range of fuel mixtures commonly encountered in natural and industrial gases.

In this investigation, a scheme with 39 species (Appendix A) and 148 elementary reactions (Appendix B) was used for a kinetic scheme represented mathematically by the set of elementary reactions:

$$\sum_{m=1}^{M} \upsilon'_{mn} \chi_m \Leftrightarrow \sum_{m=1}^{M} \upsilon''_{mn} \chi_m \quad (10)$$

Where,

υ'_{mn}, υ''_{mn} are stoichiometric coefficients of the *mth* species appearing in the reactants and products of the *nth* reaction, respectively, and X is the chemical presentation of species m taking part in the reaction.

With definition

$$\dot{C_m} = \sum_{n=1}^{N} \upsilon'_{mn} k_{rn} \prod_{m=1}^{M} [\mathrm{X}_m]^{\upsilon'_{mn}} + \sum_{n=1}^{N} \upsilon''_{mn} k_{fn} \prod_{m=1}^{M} [\mathrm{X}_m]^{\upsilon'_{mn}} \quad (11)$$

$$\dot{D_m} = \sum_{n=1}^{N} \upsilon'_{mn} k_{fn} \prod_{m=1}^{M} [\mathrm{X}_m]^{\upsilon'_{mn}} + \sum_{n=1}^{N} \upsilon''_{mn} k_{rn} \prod_{m=1}^{M} [\mathrm{X}_m]^{\upsilon''_{mn}} \quad (12)$$

The rate of production or destruction of species can be calculated as follow:

$$\dot{\rho_m} = \dot{\omega_m} W_m \tag{13}$$

$$\dot{\omega_m} = \dot{C_m} - \dot{D_m} \tag{14}$$

Where the k_{fn} and k_{rn} are forward and backward reaction rate constants and are given as follow:

$$k_{fn} = A_{fn} T^{\beta_{fn}} \exp\left(-\frac{E_{fn}}{RT}\right) \tag{15}$$

$$k_{rn} = A_{rn} T^{\beta_{rn}} \exp\left(-\frac{E_{rn}}{RT}\right) \tag{16}$$

By considering the enthalpy of the formation of each species, the heat release from the chemical reactions can therefore be calculated in each crank angle. The chemical heat release term in the energy equation is given by:

$$\dot{Q_c} = \sum_{n=1}^{N} Q_n \dot{q_n} \tag{17}$$

Where Q_n is the negative of the heat of reaction at a reference temperature, given by:

$$Q_n = \sum_{m=1}^{M} (\upsilon'_{mn} - \upsilon''_{mn})(\Delta h^{\circ}_f)_m W_m \tag{18}$$

$$\dot{q_n} = k_{fn} \prod_{m=1}^{M} [\mathrm{X}_m]^{\upsilon'_{mn}} - k_{rn} \prod_{m=1}^{M} [\mathrm{X}_m]^{\upsilon''_{mn}} \tag{19}$$

$$\dot{Q_c} = \sum_{n=1}^{N} \left[\sum_{m=1}^{M} (\upsilon'_{mn} - \upsilon''_{mn})(\Delta h^{\circ}_f)_m W_m \right]_n \dot{q_n} \tag{20}$$

$$\dot{Q_c} = - \sum_{m=1}^{M} \dot{\omega_m} (\Delta h^{\circ}_f)_m W_m \tag{21}$$

RESULTS AND DISCUSSION

In this investigation, a complete cycle simulation of the physical processes in motored engine was initially developed. For this, the Pride 1300cc engine was chosen and its data are shown in Table 1. After the zero-dimensional code had been developed, it was validated using the experimental data which were determined in the MEGA-MOTORS Company on the above engine.

TABLE 1
Engine data

Cylinder bore	7.1cm
Connecting rod	13.6cm
Stroke	8.36cm
Clearance volume	$38cm^3$
Piston cup radius	1.34cm
Inlet valve open(IVO)	14BTDC
Inlet valve close(IVC)	52ABDC
Exhaust valve open(EVO)	52BBDC
Exhaust valve close(EVC)	14ATDC
Inlet valve diameter	3.2cm
Exhaust valve diameter	2.8cm
Maximum valve lifting	8.5mm

In order to validate the quasi-dimensional code, the calculated in-cylinder pressure was compared with the experimental data presented in *Fig. 1*. The calculated pressure is in good agreement with the experimental data and the prepared program can be used for other studies in motored engine. *Fig. 2* shows the variations of the temperature and pressure of the in-cylinder gas of a Pride engine through its operating cycle. The detailed chemical kinetic mechanism was coupled with the zero-dimensional code after its validation and the results were extracted in three cases:

1. Constant pressure
2. Constant volume
3. In a motored engine

Fig. 3 shows the bulk temperature variation in a constant pressure case. The temperature rise at the ignition point shows the start of CNG combustion and this combustion will continue up to the equilibrium point, where the maximum temperature will be obtained. In this investigation, the experimental data derived by Zhou *et al.* (1993) were used to validate the calculated data. *Figs. 4* and *5* show the variations of H_2O, H_2, CO and CO_2 species concentrations with equivalence ratio. A good agreement was obtained between the calculated concentrations and the experimental data, and the maximum error is about 2 percent in these curves.

The auto-ignition time variation with equivalence ratio is shown in *Fig. 6*. As depicted in the figure, a good agreement is shown between the model and experimental data in the range of spark ignition engines operation (0.8~1.4). With the increasing equivalence ratio, the initial mass of the natural gas in the mixture increases and the auto-ignition time decreases. *Fig. 7* shows the equilibrium temperature variations with the equivalence ratio and the maximum temperature is obtained at the stoichiometric condition ($\varphi \sim 1.0$). *Figs. 8, 9* and *10* show the important effects of the parameters (initial temperature, initial pressure and equivalence ratio) on the auto-ignition time in either constant volume or constant pressure. With the increase in all the three parameters T_i, P_i and φ, the auto-ignition time decreases but the effect of the initial temperature on the auto-ignition is very important because the dependence of the reaction rates on temperature is high. With the increase in the initial temperature, the kinetic energy of the species and the number of collisions between species also increases rapidly, while the combustion starts much earlier than the other cases. Nevertheless, it is crucial to noted increasing the intake temperature will decrease the volumetric efficiency and output power of the engine.

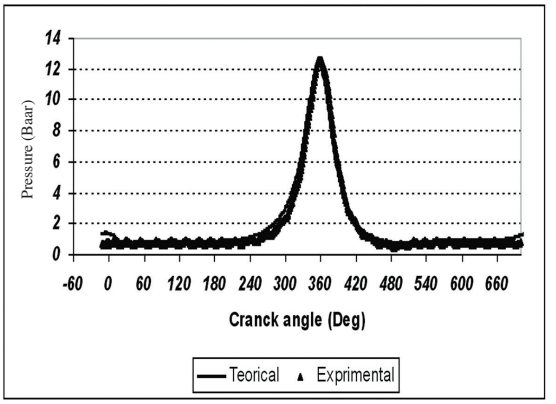

Fig. 1: The comparison between the calculated in-cylinder pressure and the experimental data

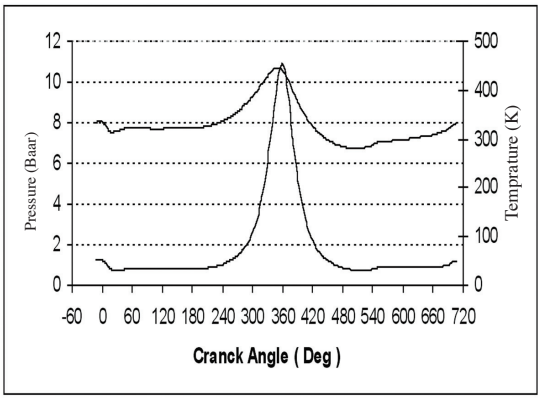

Fig. 2: Variation of calculated in-cylinder pressure and temperature through the engine cycle

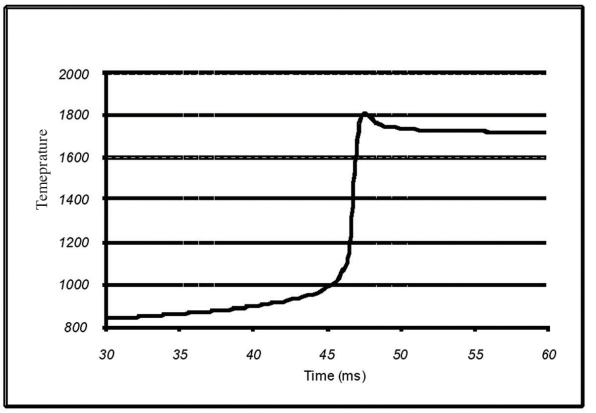

Fig. 3: Variation of temperature in constant pressure with considering the chemical kinetic vs. time at equivalence ratio (φ=2.5)

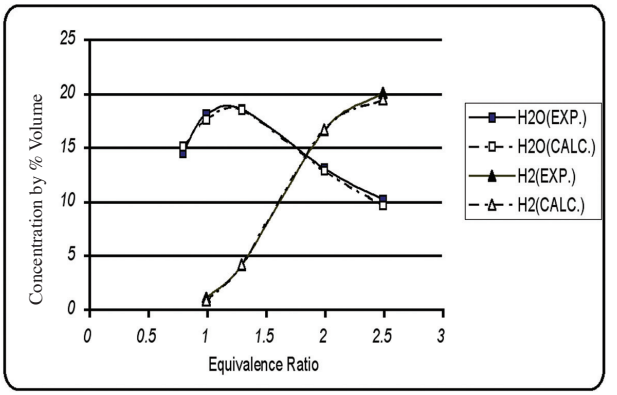

Fig. 4: Comparison of calculated concentration of H_2O, H_2 species with experimental data at constant pressure vs. equivalence ratio

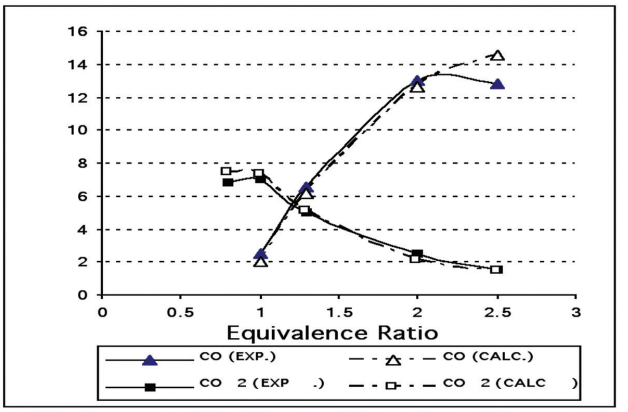

Fig. 5: Comparison of calculated concentration of CO_2, CO species with experimental data at constant pressure vs. equivalence ratio

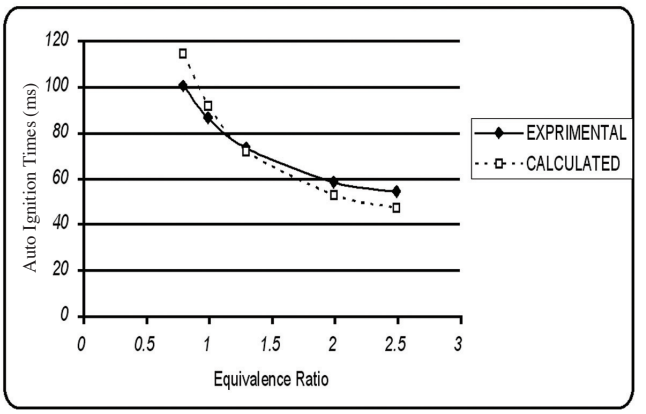

Fig. 6: Effect of equivalence ratio on auto-ignition time in constant pressure

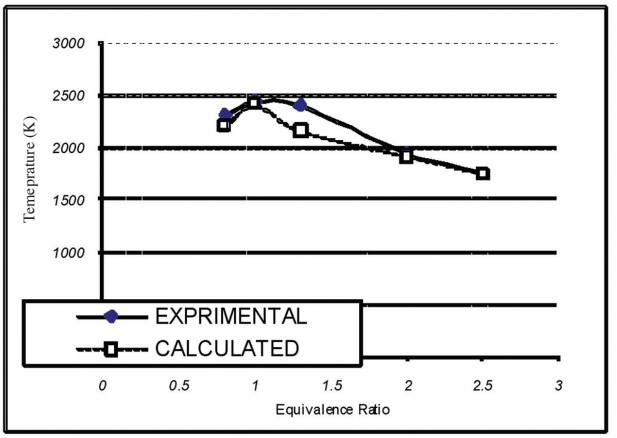

Fig. 7: Variation of equilibrium temperature after combustion with equivalence ratio

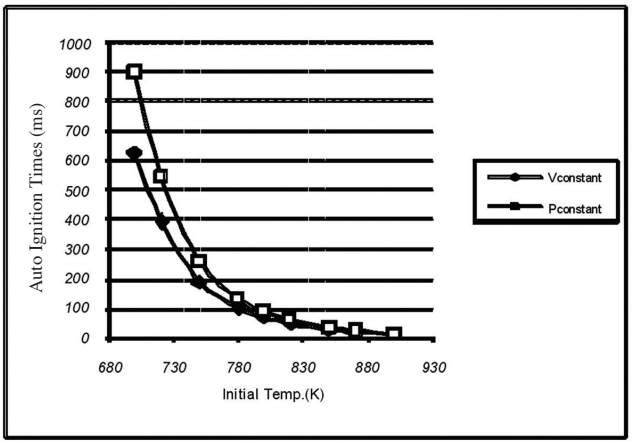

Fig. 8: Effect of initial temperature on auto-ignition time

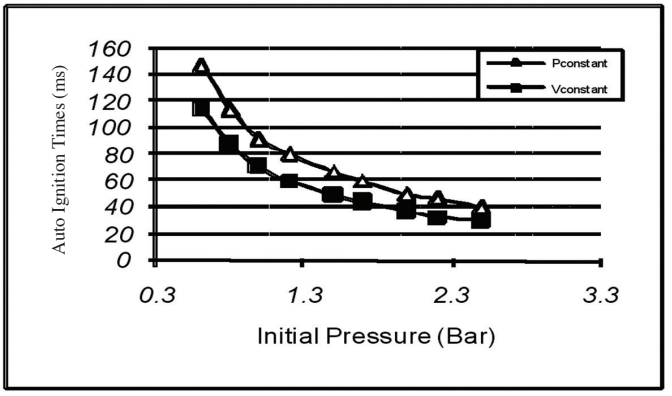

Fig. 9: Effect of initial pressure on auto-ignition time

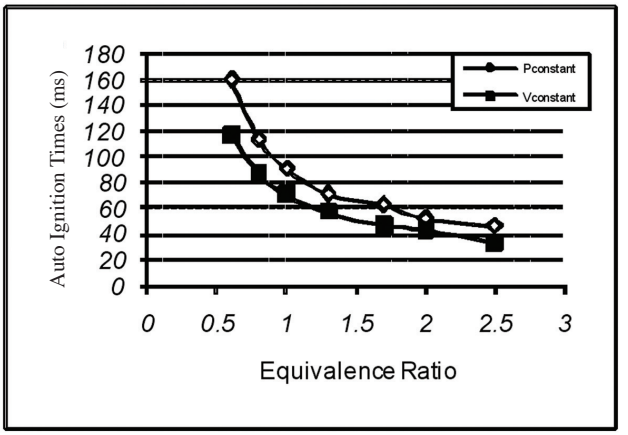

Fig. 10: Effect of equivalence ratio on auto-ignition time

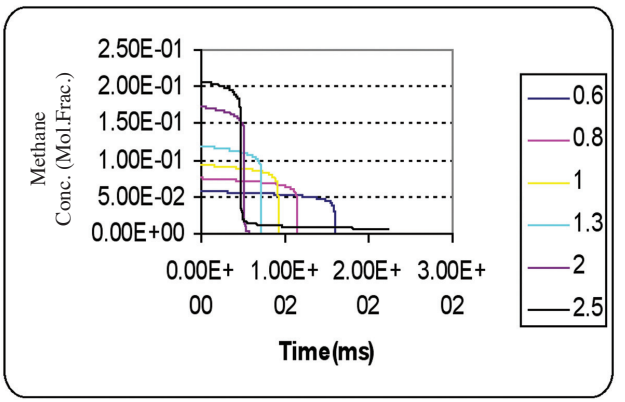

Fig. 11: Variation of CH4 concentration versus time at different equivalence ratios

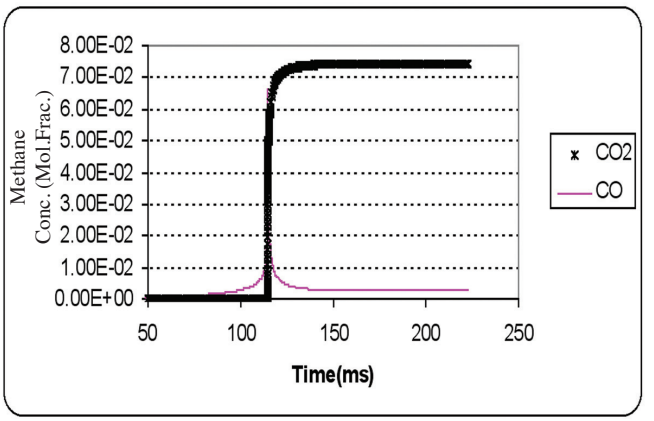

Fig. 12: Variation of CO2 and CO concentration with time in the combustion chamber (Lean mixture φ=0.8)

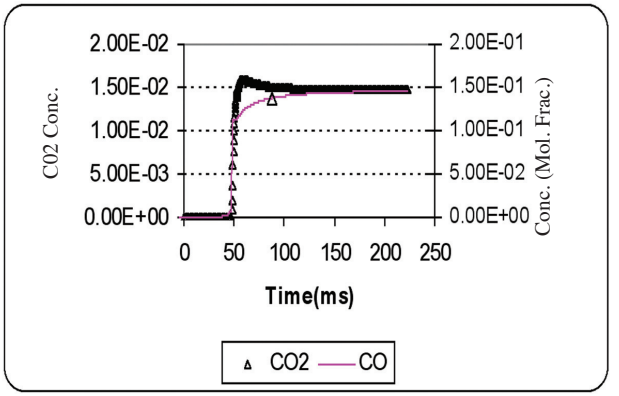

Fig. 13: Variation of CO_2 and CO concentration with time in the combustion chamber (Rich mixture φ=2.5)

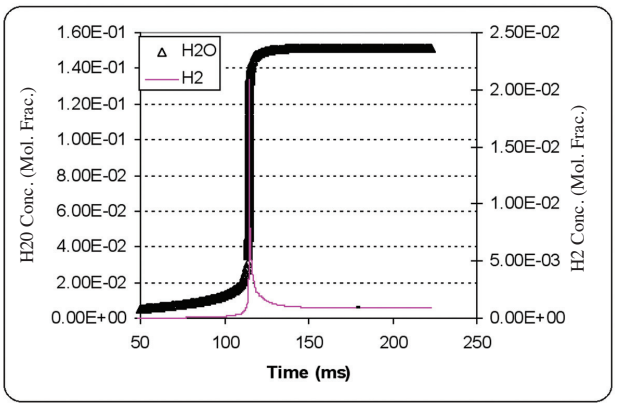

Fig. 14: Variation of H_2O and H_2 concentration with time in the combustion chamber (Lean mixture φ=0.8)

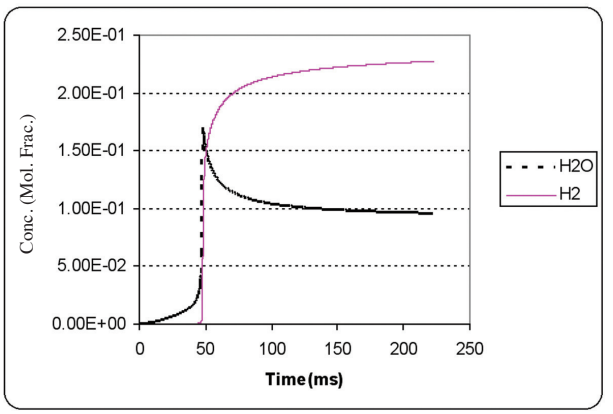

Fig. 15: Variation of H_2O and H_2 concentration with time in the combustion chamber (Rich mixture φ=2.5)

Fig. 11 shows the CH_4 concentration with time at different equivalence ratios. The sudden decrease of methane mass indicates the start of combustion and the auto-ignition point; this shows that the method can be used as a criterion to detect the auto-ignition. *Fig. 12* shows the variation of CO and CO_2 concentrations with time. It was found that the CO value increased rapidly at the start of combustion, but after the combustion completion, the oxidation of CO had taken more speed and its concentration would therefore decrease. Similarly, the CO_2 concentration will increase through oxidation of CO. *Fig. 13* shows the variation of both the CO and CO_2 concentrations in a rich mixture. Meanwhile, *Figs. 14* and *15* show the variation of H_2O and H_2 species in the lean and rich mixtures.

The nitrogen oxides (NOx) are important pollutants in internal combustion engines. The variation of nitrogen oxides (NO_x) are shown in *Fig. 16*. At the stoichiometric point, the concentrations took the maximum values and this was a result of higher combustion temperature at this condition. When the mixture is richer, the concentration of oxygen decreases, while the maximum temperature as well as the concentrations of NOx will decrease, whereas, when the mixture is leaner, the maximum temperature decreases. The variations of OH, H and O concentrations with equivalence ratio are shown in *Fig. 17*. In the combustion of methane–oxygen mixture, the OH radical has important role than H radical; while in the combustion of methane, air the role of H radical is further. This is shown in *Fig. 17*, in which the rich mixture in the production of H radical is further than the OH radical. The stable intermediate species of C_2H_2, C_2H_4 and C_2H_6 concentration variations with equivalence ratio are shown in *Fig. 18*, while some concentration variations of species are shown in *Fig. 19*. Using the detailed chemical kinetic presented for the motoring cycle of an engine (1300cc), a part of pressure and temperature rise of in-cylinder gas can be from the heat release from the chemical reactions in each crank angle. In each crank angle, the following can therefore be written:

$$\Delta P \text{ (total)} = \Delta P \text{ (piston motion)} + \Delta P \text{ (heat release from chemical reactions)} \quad (22)$$

$$\Delta T \text{ (total)} = \Delta T \text{ (piston motion)} + \Delta T \text{ (heat release from chemical reactions)} \quad (23)$$

The rise in pressure and temperature at the ignition point can be used as the criteria to detect that particular point. *Figs. 20* and *21* compare the pressure and temperature variations in a motored engine with the application of detailed chemical kinetic and without its application. The separation of the curves at the ignition point is illustrated in the figures.

The variations of ΔT and ΔP, adjusted with the heat release from the chemical kinetic reactions, are shown in *Fig. 22*. When the combustion was started at ignition point, the values of ΔT and ΔP increased rapidly. The effect of compression ratio on ΔP is shown in *Fig. 23*; the increase in the compression ratio caused the ΔP to increase. The variations in the temperature of the in-cylinder gas are shown in *Fig. 24* at two different equivalence ratios. This figure shows that no combustion occurs at this compression ratio and pressure. As discussed in the earlier section, the initial temperature is one of the important parameters which greatly affects the auto-ignition time. *Fig. 25* shows the effect of the initial mixture temperature on the auto-ignition on the pressure curve at same compression ratios and other engine operating parameters. When the temperature is increased, the activation energy will also increase and the ignition occurs at the early stage of the compression.

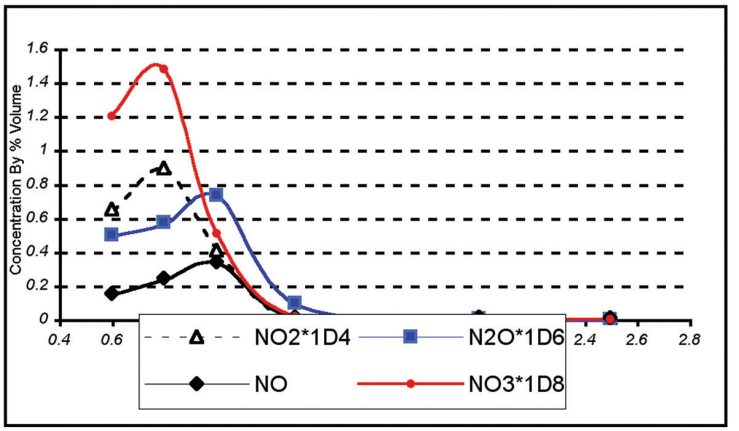

Fig. 16: Variation of nitrogen oxides (NOx) concentrations with equivalence ratio

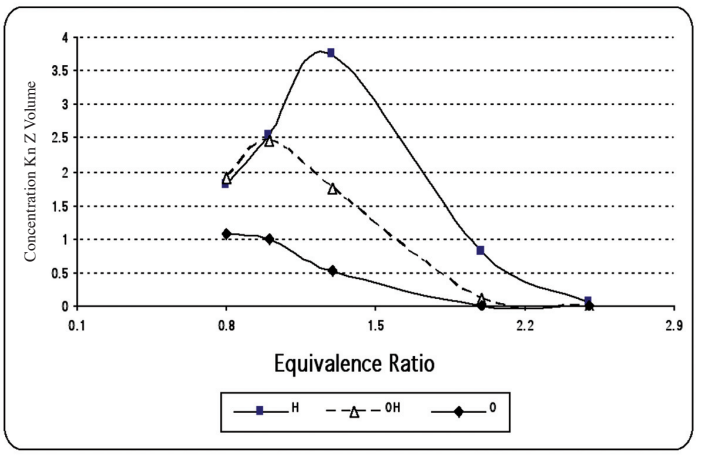

Fig. 17: Variation of H, OH and O radicals values with equivalence ratio

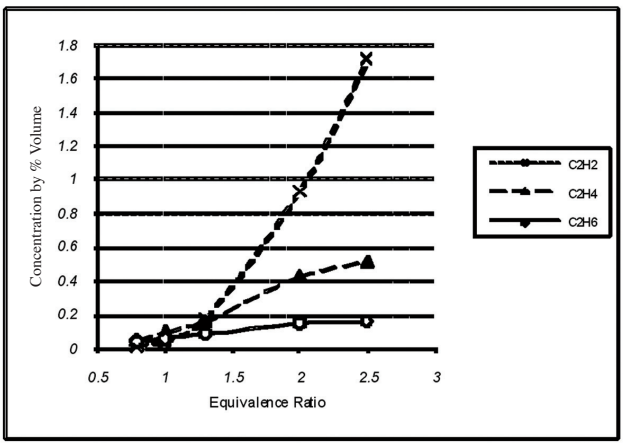

Fig. 18: Variation of intermediate species C_2H_2, C_2H_4 and C_2H_8 with equivalence ratio

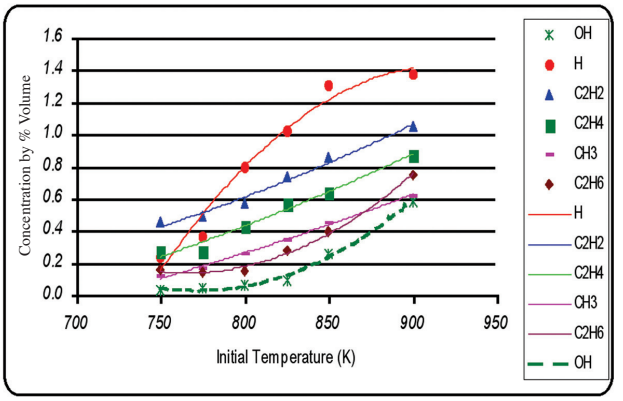

Fig. 19: Variation of some species with initial temperature

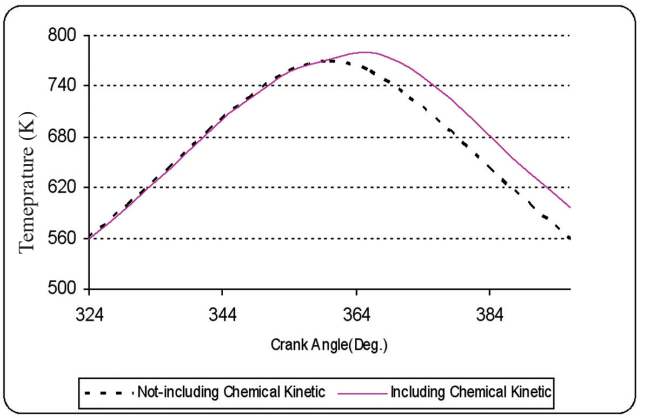

Fig. 20: Variation of in-cylinder gas bulk temperature vs. crank angle

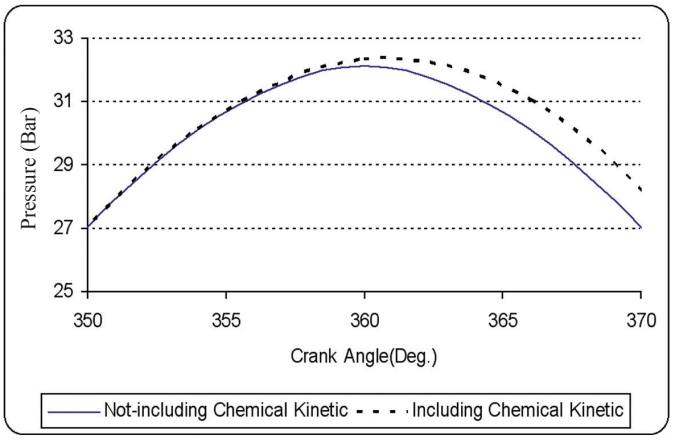

Fig. 21: Variation of in-cylinder gas pressure vs. crank angle

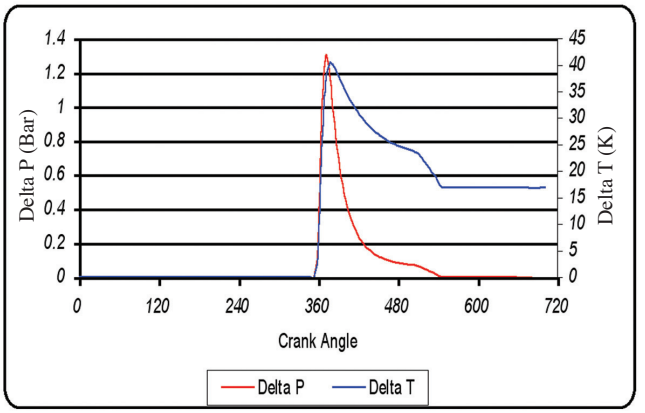

Fig. 22: Variation of ΔP and ΔT with crank angle

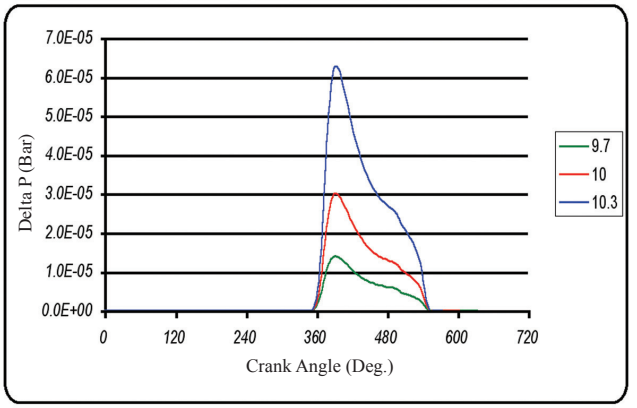

Fig. 23: Variation of ΔP with crank angle at different compression ratios

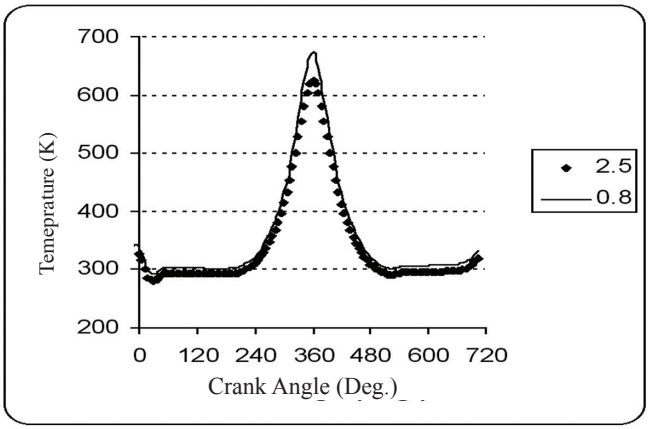

Fig. 24: Variation of in-cylinder gas bulk temperature with crank angle at different equivalence ratios

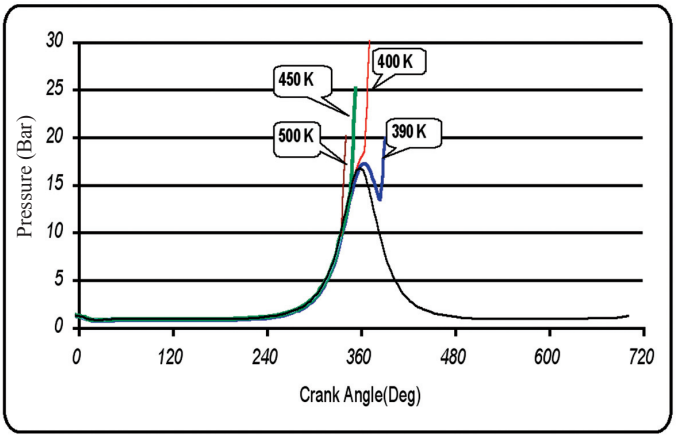

Fig. 25: Variation of in-cylinder pressure to show the effect of initial temperature on auto-ignition time

CONCLUSIONS

An in-house quasi-dimensional code was developed to simulate the physical processes of a CNG engine, in conjunction with a detailed chemical kinetic scheme, to predict the auto-ignition condition of that particular engine. In this study, the calculated results were found to have a good agreement with the experimental data. In more specific, the prepared code can be used to predict the auto-ignition point in the CNG engine satisfactory. Similarly, this code can also be used in parametric study to show the effects of important design and operating parameters on auto-ignition time.

REFERENCES

Bade Shrestha S.O. (1999). A predictive model for gas fueled spark ignition engine application. PhD. Thesis, Department of Mechanical Engineering, University of Calgary, Canada.

Bakhshan, Y., Karim, G.A. and Mansouri, S.H. (2002). Unsteady Heat Transfer during the Rapid Compression and Expansion of Air. ASME paper ETCE2002/CAE-29015.

Bakhshan, Y. and Mansouri, S.H. (2003). Comparison between zero and multi-dimensional turbulence models for internal combustion engine application. In *Proceeding of ISME2003*, Mashad, Iran.

Bakhshan, Y., Karim, G.A. and Mansouri, S.H. (2003). Study of instantaneous unsteady heat transfer in a rapid-compression-expansion machine using zero-dimensional turbulence model. Accepted for publication in Iranian Journal of Science and Technology, Shiraz, Iran.

Emad Boshra Fawzy Khalil. (2000). Modelling the chemical kinetic of combustion of higher hydrocarbon fuels in air. Ph.D. Thesis, Department of Mechanical Engineering, University of Calgary, Canada.

Heywood, J.B. (1988). *Internal Combustion Engine Fundamental.* New York: McGraw-Hill.

Higgin, R. and William, A. (1969). A shock tube investigation of the ignition of lean methane and n-Butane mixtures with oxygen. In *12th Symposium (International) on Combustion* (p. 579), the Combustion Institute, Pittsburg, Pa.

Jenning, M.J. and Jeske, F.R. (1994). Analysis of the injection process in direct injected natural gas engines:part II Effects of injector and combustion chamber design. *J. Eng. Gas. Turb. Power*, *116,* 806-813.

Jenning, M.J. and Jeske, F.R. (2004). Analysis of the injection process in direct injected natural gas engines:part I study of unconfined and in cylinder plume behavior. *J. Eng. Gas. Turb. Power*, *116,* 799-805

Karim, G.A. (2002). *Personal Communications*.

Karim, G.A., Hanafi, A. and Zhou, G. (1992). A kinetic investigation of the oxidation of low heating value fuel mixtures of methane and diluents. In *Proceeding of the 15th Annual ASME/ETCE*, Houston, Texas.

Khalil, E., Samuel, P. and Karim, G.A. (1996). An analytical examination of chemical kinetic of the combustion of n-heptane-methane air mixtures. SAE Paper No.961932.

Mansouri, S.H. and Bakhshan, Y. (2000). The k-epsilon Turbulence modelling of heat transfer and Combustion processes in a Texaco Controlled Combustion Stratified Charge Engine. *Journal of Automobile Engineering, ImechE,* PartD, *214*.

Mansouri, S.H. and Bakhshan, Y. (2001). Studies of Nox, CO, Soot formation and oxidation from direct-injection Stratified-Charge Engine Using k-epsilon Turbulence Model. *Journal of Automobile Engineering*, ImechE, PartD, *215*, UK.

Mansouri, S.H. and Heywood, J.B. (1980). Correlation for the viscosity and Prandtl number of hydrocarbon -air combustion products. *Combust. Sci.Technology*, *23,* 251-256.

Mansouri, S.H. and Bakhshan, Y. (2000). Prediction of soot formation and oxidation in a direct-injection Stratified-Charge Engine. *Proceeding of ISME2001*, Sharif University of Technology, Tehran, Iran.

Mozaffari, A., Bakhshan, Y. and Agdasi, N. (2003). Simulation of methane combustion with using detailed chemical kinetic. In *Proceeding of ISME2003*, Mashad, Iran.

Papageorgakis, G.C. (1997). Turbulence modelling of gaseous injection and mixing in DI engines. Ph.D Thesis, Ann Arbor, Michigan.

Papageorgakis, G.C. and Dennis, N.A. (1998). Optimizing gaseous fuel-air mixing direct injection engines using an RNG based model. SAE Paper 980135.

Ramos, J.I. (1988). *Internal Combustion Engine Modelling*. New York: Hemisphere Pub. Corp.

Turns, S.R. (1996). *An Introduction to Combustion*. McGraw-Hill.

Westbrook, C.K. and Pitz, W.J. (1998). Detailed kinetic modelling of auto ignition chemistry. *Transacation of SAE*, *96*(7), 559.

Zhou, G.R. (1993). Analytical studies of methane combustion and the production of hydrogen and/or synthesis gas by thr uncatalysed partical oxidation of methane. Ph.D. Thesis, Department of Mechanical Engineering, University of Calgary, Canada.

APPENDIX A
Chemical species considered in this investigation

No.	Species	Chemical	Molecular
1	Methane	CH_4	16.043
2	Ethynyl	C_2H	25.0303
3	Acetylene	C_2H_2	26.0382
4	Vinyl	C_2H_3	27.0462
5	Ethylene	C_2H_4	28.0542
6	Ethyl	C_2H_5	29.0622
7	Ethane	C_2H_6	30.0701
8	Methylidene	CH	13.0191
9	Methylene	CH_2	14.0270
10	Ketene	CH_2CO	42.0376
11	Formaldehyde	CH_2O	30.0265
12	Methyl	CH_3	15.0351
13	Acetaldehyde	CH_3CHO	44.0536
14	Acetyl	CH_3CO	43.0456
15	Methyloxide	CH_3O	31.0345
16	Ketyl	CHCO	41.0297
17	Carbon Monoxide	CO_2	28.0106
18	Carbon Dioxide	CO	44.0100
19	Hydrogen Atom	H	1.00797
20	Hydrogen Molecule	H_2	2.01594
21	Steam	H_2O	18.0153
22	Hydrogen Peroxide	H_2O_2	34.0147
23	Formyl	HCO	29.0185
24	Hydroperoxo	HO_2	33.0068
25	Oxygen	O_2	31.9988
26	Oxygen Atom	O	15.9994
27	Hydroxyl	OH	17.0074
28	Carbon	C	12.0110
29	Cyanogen	CN	26.0180
30	Nitrogen	N_2	28.0134
31	Nitrogen Atom	N	14.0067
32	Hydrogen Cyanide	HCN	27.0260
33	Hydrogen Isocyanate	HCNO	43.0250
34	Nitric Acid	HNO_3	63.0130
35	Imidogen	NH	15.0150
36	Nitrogen Oxide	NO	30.0060
37	Nitrogen Dioxide	NO_2	46.0060
38	Nitrous Oxide	N_2O	44.0130
39	Nitrogen Trioxide	NO_3	62.0050

APPENDIX B
Chemical Kinetics Reactions Mechanism (SI Units)

No.	Chemical Reactions	A_{fn}	β_{fn}	E_{fn}	A_{rn}	β_{rn}	E_{rn}
1	$CH_4 + OH \Leftrightarrow CH_3 + H_2O$	2.200E+07	0.000	2.093E+03	3.750E+06	0.000	9.251E+04
2	$CH_4 + H \Leftrightarrow CH_3 + H_2$	6.900E+07	0.000	4.940E+04	2.480E+07	0.000	5.986E+04
3	$CH_4 + O \Leftrightarrow CH_3 + OH$	1.000E+07	0.000	3.374E+04	1.550E+05	0.000	3.375E+04
4	$CH_4 + HO_2 \Leftrightarrow CH_3 + H_2O_2$	2.000E+07	0.000	7.535E+04	1.050E+06	0.000	6.061E+04
5	$CH_4 + O_2 \Leftrightarrow CH_3 + HO_2$	1.000E+07	0.000	2.300E+05	1.480E+06	0.000	-1.126E+03
6	$CH_4 \Leftrightarrow CH_3 + H$	1.000E+15	0.000	4.200E+05	1.026E+05	0.000	-7.100E+04
7	$CH_3 + O \Leftrightarrow HCO + H_2$	1.000E+08	0.000	0.000E+00	9.372E+07	0.000	3.943E+05
8	$CH_3 + O \Leftrightarrow CH_2O + H$	1.300E+08	0.000	8.400E+03	1.590E+09	0.000	2.901E+05
9	$CH_3 + O_2 \Leftrightarrow CH_2O + OH$	1.000E+05	0.000	0.000E+00	8.450E+04	0.000	2.117E+05
10	$CH_3 + OH \Leftrightarrow CH_2O + H_2$	8.000E+06	0.000	0.000E+00	2.940E+09	-0.300	3.043E+05
11	$CH_3 + O_2 \Leftrightarrow CH_3O + O$	4.786E+07	0.000	1.214E+05	3.019E+08	0.000	3.050E+03
12	$CH_3 + HO_2 \Leftrightarrow CH_3O + OH$	2.000E+07	0.000	0.000E+00	1.000E-06	0.000	0.000E+00
13	$CH_3 + OH \Leftrightarrow CH_3O + H$	4.520E+08	0.000	6.488E+04	4.750E+10	-0.130	8.836E+04
14	$CH_3 + CH_3 \Leftrightarrow C_2H_4 + H_2$	5.000E+09	0.000	1.339E+05	1.540E+14	-0.750	3.794E+05
15	$CH_3 + CH_3 \Leftrightarrow C_2H_5 + H$	2.400E+09	0.000	1.113E+05	3.210E+48	10.770	1.650E+05
16	$CH_3 + CH_3 \Leftrightarrow C_2H_6$	6.830E+16	-3.36	5.774E+03	3.680E+34	-5.730	3.893E+05
17	$CH_3 + NO_2 \Leftrightarrow CH_3O + NO$	1.300E+07	0.000	0.000E+00	2.460E+07	0.000	7.535E+04
18	$CH_3 + OH \Leftrightarrow CH_2 + H_2O$	7.500E+00	2.000	2.093E+04	4.980E+07	0.000	7.610E+04
19	$CH_3 + H \Leftrightarrow CH_2 + H2$	9.000E+07	0.000	6.312E+04	1.500E+07	0.000	4.113E+04
20	$CH3 + N \Leftrightarrow H + H + HCN$	5.000E+07	0.000	0.000E+00	5.058E+06	0.000	4.644E+04
21	$CH2O + OH \Leftrightarrow HCO + H2O$	3.390E+03	1.200	-1.64E+03	1.180E+07	0.000	1.319E+05
22	$CH2O + H \Leftrightarrow HCO + H2$	1.000E+08	0.000	1.920E+04	7.420E+08	0.000	1.338E+05
23	$CH2O + O \Leftrightarrow HCO + OH$	1.000E+08	0.000	2.220E+04	1.000E+08	0.000	1.460E+05
24	$CH2O + M \Leftrightarrow HCO + H + M$	3.310E+10	0.000	3.389E+05	1.410E-01	1.000	-4.92E+04
25	$CH2O + CH3 \Leftrightarrow HCO + CH4$	1.000E+04	0.500	2.512E+04	2.090E+04	0.500	8.851E+04
26	$CH2O + HO2 \Leftrightarrow HCO + H2O2$	1.000E+06	0.000	3.349E+04	1.090E+05	0.000	2.760E+04
27	$CH2O + O2 \Leftrightarrow HCO + HO2$	1.000E+08	0.000	1.340E+05	2.880E+06	0.000	8.791E+03
28	$CH3O + M \Leftrightarrow CH2O + H + M$	5.000E+07	0.000	8.786E+03	9.910E-04	1.000	-1.07E+04
29	$CH3O + O2 \Leftrightarrow CH2O + HO2$	1.000E+06	0.000	2.510E+04	1.280E+05	0.000	1.346E+05
30	$HCO + OH \Leftrightarrow CO + H2O$	5.000E+07	0.000	0.000E+00	1.170E+08	-0.500	3.824E+05
31	$HCO + O2 \Leftrightarrow CO + HO2$	3.300E+07	-0.40	0.000E+00	1.878E+05	0.000	7.761E+04
32	$HCO + O \Leftrightarrow CO + OH$	3.000E+07	0.000	0.000E+00	2.880E+08	0.000	3.678E+05
33	$HCO + H \Leftrightarrow CO + H2$	7.000E+07	0.000	0.000E+00	1.310E+09	0.000	3.770E+05
34	$HCO + M \Leftrightarrow CO + H + M$	7.100E+08	0.000	7.030E+04	1.140E+03	0.000	9.980E+03
35	$HCO + O \Leftrightarrow CO2 + H$	3.000E+07	0.000	0.000E+00	9.690E+09	0.000	4.611E+05
36	$HCO + CH3 \Leftrightarrow CH4 + CO$	3.000E+05	0.500	0.000E+00	5.140E+07	0.500	3.787E+05
37	$CHCO + H \Leftrightarrow CH2 + CO$	3.000E+07	0.000	0.000E+00	6.380E-02	2.200	1.122E+05
38	$CHCO + O \Leftrightarrow CO + CO + H$	1.200E+06	0.000	0.000E+00	0.000E+00	0.000	0.000E+00
39	$C2H + O2 \Leftrightarrow CO + HCO$	1.000E+07	0.000	2.929E+04	8.900E+06	0.000	5.791E+05
40	$C2H + O \Leftrightarrow CH + CO$	5.012E+07	0.000	0.000E+00	3.160E+07	0.000	2.487E+05
41	$C2H2 + M \Leftrightarrow C2H + H + M$	1.000E+08	0.000	4.770E+05	1.110E-03	1.000	3.220E+03
42	$C2H2 + O2 \Leftrightarrow HCO + HCO$	3.980E+06	0.000	1.172E+05	1.000E+05	0.000	2.659E+05
43	$C2H2 + H \Leftrightarrow C2H + H2$	1.995E+08	0.000	7.953E+04	4.160E+07	0.000	5.527E+04
44	$C2H2 + OH \Leftrightarrow C2H + H2O$	6.310E+06	0.000	2.929E+04	5.370E+06	0.000	6.845E+04
45	$C2H2 + OH \Leftrightarrow CH2CO + H$	3.230E+05	0.000	8.370E+02	3.160E+06	0.000	8.732E+04
46	$C2H2 + O \Leftrightarrow C2H + OH$	3.230E+09	-0.60	7.113E+04	2.950E+08	-0.600	3.810E+03
47	$C2H2 + O \Leftrightarrow CH2 + CO$	6.760E+07	0.000	1.674E+04	1.250E+07	0.000	2.287E+05
48	$C2H2 + OH \Leftrightarrow CH3 + CO$	1.202E+06	0.000	2.090E+03	2.500E+06	0.000	2.427E+05
49	$C2H2 + O2 \Leftrightarrow CH2 + CO2$	6.000E+07	0.000	1.674E+05	3.400E+08	0.000	5.107E+05
50	$C2H2 + O2 \Leftrightarrow CHCO + H$	4.300E+08	0.000	5.070E+04	4.870E+11	-0.860	1.337E+05
51	$C2H3 + O2 \Leftrightarrow C2H2 + HO2$	1.585E+07	0.000	4.186E+04	1.000E+06	0.000	7.477E+04
52	$C2H3 + M \Leftrightarrow C2H2 + H + M$	7.940E+08	0.000	1.318E+05	1.230E-01	1.000	-4.33E+04
53	$C2H3 + O2 \Leftrightarrow CH2O + HCO$	1.070E+05	0.000	-1.04E+03	4.470E-25	8.340	2.935E+05
54	$C2H3 + H \Leftrightarrow C2H2 + H2$	2.000E+07	0.000	0.000E+00	3.850E-19	7.390	2.137E+05

55	C2H4 + OH ⇔ C2H3 + H2O	4.786E+06	0.000	5.150E+03	1.200E+06	0.000	5.560E+04
56	C2H4 + H ⇔ C2H3 + H2	1.514E+01	2.000	2.511E+04	1.730E+00	2.000	2.138E+04
57	C2H4 + M ⇔ C2H3 + H + M	3.800E+11	0.000	4.107E+05	2.000E+05	0.000	0.000E+00
58	C2H4 + M ⇔ C2H2 + H2 + M	2.600E+11	0.000	3.320E+05	4.600E+00	1.000	1.528E+05
59	C2H4 + OH ⇔ CH2O + CH3	2.000E+06	0.000	4.002E+03	6.000E+05	0.000	6.899E+04
60	C2H4 + O ⇔ CH3 + HCO	1.600E+03	1.200	3.096E+03	1.600E-03	2.370	1.061E+05
61	C2H4 + O ⇔ CH2 + CH2O	2.500E+07	0.000	2.092E+04	3.020E+06	0.000	6.564E+04
62	C2H4 + C2H4 ⇔ C2H3 + C2H5	5.012E+08	0.000	2.708E+05	1.490E+08	0.000	-1.09E+04
63	C2H5 ⇔ C2H4 + H	2.340E+26	-4.24	1.810E+05	1.170E+08	-0.620	7.238E+03
64	C2H5 + O2 ⇔ C2H4 + HO2	1.000E+06	0.000	2.093E+04	1.300E+05	0.000	5.732E+04
65	C2H5 + O ⇔ CH3CHO + H	5.000E+07	0.000	0.000E+00	5.360E-01	2.540	2.893E+05
66	C2H6 + H ⇔ C2H5 + H2	5.400E-04	3.500	2.180E+04	9.720E-04	3.500	1.143E+05
67	C2H6 + OH ⇔ C2H5 + H2O	6.300E+00	2.000	2.700E+03	9.780E+29	-6.550	1.627E+05
68	C2H6 + O ⇔ C2H5 + OH	3.000E+01	2.000	2.140E+04	6.940E+28	-6.320	1.078E+05
69	C2H6 + CH3 ⇔ C2H5 + CH4	5.500E-07	4.000	3.470E+04	2.291E+08	0.000	1.001E+05
70	CO + O2 ⇔ CO2 + O	3.140E+05	0.000	1.573E+05	1.900E+07	0.000	2.266E+05
71	CO + OH ⇔ CO2 + H	4.400E+00	1.500	-3.09E+03	1.380E+08	0.000	1.072E+05
72	CO + O + M ⇔ CO2 + M	5.900E+03	0.000	1.716E+04	5.500E+15	-1.000	5.516E+05
73	CO + HO2 ⇔ CO2 + OH	5.800E+07	0.000	9.581E+04	6.600E+08	0.000	3.546E+05
74	CH2 + O2 ⇔ HCO + OH	1.000E+08	0.000	1.549E+04	4.070E+07	0.000	3.204E+05
75	CH2 + O ⇔ CH + OH	1.900E+05	0.680	1.046E+05	5.860E+04	0.680	1.085E+05
76	CH2 + H ⇔ CH + H2	2.512E+05	0.670	1.076E+05	1.900E+05	0.670	1.201E+05
77	CH2 + OH ⇔ CH + H2O	2.512E+05	0.670	1.076E+05	8.120E+05	0.670	1.836E+05
78	CH2 + CH3 ⇔ C2H4 + H	4.000E+07	0.000	0.000E+00	4.380E+10	0.000	2.466E+05
79	CH2 + O ⇔ CO + H + H	5.000E+07	0.000	0.000E+00	0.000E+00	0.000	0.000E+00
80	CH2 + O2 ⇔ CO + H + OH	8.640E+04	0.000	-2.09E+03	2.270E-07	1.550	2.284E+05
81	CH2 + O2 ⇔ CO + H2O	1.870E+04	0.000	-4.18E+03	3.070E+00	1.400	7.276E+05
82	CH2 + O2 ⇔ CO2 + H + H	1.590E+06	0.000	4.184E+03	3.010E+01	0.230	3.442E+05
83	CH2 + NO ⇔ HCNO + H	1.390E+06	0.000	-4.61E+03	2.340E+08	0.000	-1.04E+05
84	CH2 + N2 ⇔ HCN + NH	2.800E+06	0.000	1.256E+05	6.800E+05	0.000	0.000E+00
85	CH2 + NO ⇔ HCN + OH	1.390E+06	0.000	-4.61E+03	1.658E+06	0.000	2.581E+05
86	CH + NO ⇔ HCN + O	1.100E+08	0.000	0.000E+00	2.600E+09	0.000	2.971E+05
87	CH + N2 ⇔ HCN + N	8.000E+05	0.000	4.605E+04	7.200E+06	0.000	3.893E+04
88	CH + H2O ⇔ CH2O + H	1.170E+09	-.750	0.000E+00	1.512E+08	0.000	2.396E+05
89	CH + CO2 ⇔ HCO + CO	3.400E+06	0.000	2.888E+03	4.200E+05	0.000	2.752E+05
90	CH + H ⇔ C + H2	1.500E+08	0.000	0.000E+00	5.300E+08	0.000	9.617E+04
91	CH + O2 ⇔ CO + OH	1.349E+05	0.670	1.075E+05	5.120E+05	0.670	7.766E+05
92	CH + O2 ⇔ HCO + O	1.000E+07	0.000	0.000E+00	1.340E+07	0.000	3.010E+05
93	CH + O ⇔ CO + H	4.000E+07	0.000	0.000E+00	5.490E+08	0.150	7.343E+05
94	CH2CO + H ⇔ CH3 + CO	1.096E+07	0.000	1.423E+04	2.399E+06	0.000	1.682E+05
95	CH2CO + O ⇔ HCO + HCO	1.000E+07	0.000	1.004E+04	3.467E+05	0.000	1.402E+05
96	CH2CO + OH ⇔ CH2O + HCO	2.818E+07	0.000	0.000E+00	2.754E+07	0.000	7.740E+04
97	CH2CO + M ⇔ CH2 + CO + M	1.995E+10	0.000	2.510E+05	4.572E-02	0.000	0.000E+00
98	CH3CHO + H ⇔ CH3CO + H2	4.000E+07	0.000	1.760E+04	8.420E+10	-1.370	9.719E+04
99	CH3CHO + O ⇔ CH3CO + OH	5.000E+06	0.000	7.500E+03	7.390E+09	-1.420	7.979E+04
100	CH3CHO + OH ⇔ CH3CO + H2O	1.000E+07	0.000	0.000E+00	9.910E+11	-1.650	1.459E+05
101	CH3CO ⇔ CH3 + CO	1.000E+10	0.000	0.000E+00	0.000E+00	0.000	0.000E+00
102	H2 + OH ⇔ H + H2O	2.200E+07	0.000	2.155E+04	9.300E+07	0.000	8.490E+04
103	H2 + O ⇔ H + OH	1.800E+04	1.000	3.711E+04	8.300E+03	1.000	2.890E+05
104	H2 + O2 ⇔ OH + OH	1.360E+07	0.000	2.015E+05	4.480E+05	0.000	1.253E+05
105	H2 + HO2 ⇔ H + H2O2	7.300E+05	0.000	7.820E+04	1.700E+06	0.000	1.540E+04
106	H + HO2 ⇔ OH + OH	2.500E+08	0.000	7.500E+03	1.200E+07	0.000	1.630E+05
107	H + H + M ⇔ H2 + M	6.400E+05	-1.00	0.000E+00	2.400E+09	0.000	4.812E+05
108	H + OH + M ⇔ H2O + M	1.413E+11	-2.00	0.000E+00	2.200E+10	0.000	4.390E+05
109	H + O2 + M ⇔ HO2 + M	1.590E+03	0.000	-4.18E+03	2.400E+09	0.000	1.921E+05
110	O + O + M ⇔ O2 + M	4.700E+03	-0.28	0.000E+00	5.100E+09	0.000	4.810E+05
111	H2O2 + M ⇔ OH + OH + M	1.690E+18	-2.00	2.023E+05	3.250E+10	-2.000	0.000E+00
112	HO2 + OH ⇔ H2O + O2	5.000E+07	0.000	4.180E+03	1.000E+08	0.000	3.091E+06
113	HO2 + HO2 ⇔ H2O2 + O2	1.000E+07	0.000	4.200E+03	6.800E+07	0.000	1.782E+05
114	H2O2 + H ⇔ H2O + OH	3.200E+08	0.000	3.751E+04	1.140E+03	1.360	3.176E+05

115	H + O2 ⇔ OH + O	1.200E+11	-0.91	6.910E+04	1.300E+07	0.000	0.000E+00
116	H2O + O ⇔ OH + OH	1.500E+04	1.140	7.213E+04	1.500E+03	1.140	0.000E+00
117	OH + M ⇔ H + O + M	8.000E+13	-1.00	4.339E+05	1.000E+04	0.000	0.000E+00
118	HO2 + H ⇔ H2 + O2	2.500E+07	0.000	2.929E+03	5.000E+08	-0.280	2.243E+05
119	HO2 + O ⇔ O2 + OH	2.000E+07	0.000	0.000E+00	2.810E+08	-0.330	2.141E+05
120	H2O2 + OH ⇔ H2O + HO2	1.000E+07	0.000	7.531E+03	2.800E+07	0.000	1.372E+05
121	C + N2 ⇔ CN + N	3.624E+02	0.000	1.591E+05	1.040E+09	-0.500	0.000E+00
122	C + NO ⇔ CN + O	6.600E+07	0.000	0.000E+00	7.300E+13	0.000	1.588E+05
123	C + N2O ⇔ CN + NO	1.000E+07	0.000	0.000E+00	1.330E+12	0.000	3.454E+05
124	C + O2 ⇔ CO + O	2.000E+07	0.000	0.000E+00	4.182E+07	0.000	5.793E+05
125	CN + OH ⇔ NH + CO	6.000E+06	0.000	0.000E+00	1.600E+07	0.000	2.512E+05
126	CN + O2 ⇔ NO + CO	6.000E+06	0.000	0.000E+00	6.800E+06	0.000	4.605E+05
127	CN + H2 ⇔ H + HCN	2.950E-01	2.450	9.364E+03	6.587E+03	0.000	8.037E+04
128	HCN + O ⇔ NH + CO	3.450E-03	2.640	2.085E+04	2.110E+06	0.000	1.646E+05
129	HCNO + H ⇔ HCN + OH	1.000E+08	0.000	5.023E+04	4.210E+06	0.000	-4.79E+03
130	HNO3 + OH ⇔ NO3 + H2O	5.400E+04	0.000	0.000E+00	2.446E+08	0.000	3.271E+05
131	NH + H ⇔ N + H2	1.000E+08	0.000	0.000E+00	4.536E+08	0.000	1.222E+05
132	N + NO ⇔ O + N2	3.270E+06	0.300	0.000E+00	1.670E+08	0.000	3.174E+05
133	N + O2 ⇔ O + NO	6.400E+03	1.000	2.629E+04	3.880E+06	0.000	1.666E+05
134	N + OH ⇔ H + NO	3.800E+07	0.000	0.000E+00	1.200E+08	0.000	2.024E+05
135	NO + HO2 ⇔ NO2 + OH	8.700E+05	0.000	0.000E+00	6.000E+06	0.000	3.349E+04
136	NO + O + M ⇔ NO2 + M	5.800E-02	1.000	-3.60E+04	1.100E+10	0.000	2.721E+05
137	NO + NO + O2 ⇔ NO2 + NO2	4.900E-06	1.000	-2.51E+03	4.000E+06	0.000	1.130E+05
138	NO + O2 + M ⇔ NO3 + M	7.650E-06	1.000	-7.11E+03	1.200E+05	0.000	1.340E+04
139	NO + NH ⇔ N2O + H	4.300E+08	-0.50	0.000E+00	2.575E+04	0.000	-1.65E+05
140	NO + NO ⇔ N2 + O2	1.410E+09	0.000	3.558E+05	2.850E+10	0.000	5.358E+05
141	NO2 + H ⇔ NO + OH	2.900E+07	0.000	0.000E+00	3.500E+05	0.000	1.231E+05
142	NO2 + O ⇔ NO + O2	1.000E+07	0.000	2.512E+03	2.200E+06	0.000	1.926E+05
143	NO2 + OH + M ⇔ HNO3 + M	9.305E+04	0.000	-7.27E+04	6.000E+08	0.000	1.260E+05
144	N2O + M ⇔ N2 + O + M	1.600E+08	0.000	2.159E+05	8.373E+10	0.000	3.750E+06
145	N2O + O ⇔ NO + NO	1.000E+08	0.000	1.180E+05	2.254E+06	0.000	2.744E+05
146	N2O + H ⇔ N2 + OH	7.600E+07	0.000	6.363E+04	2.778E+06	0.000	3.342E+05
147	NO3 + NO ⇔ NO2 + NO2	1.500E+04	0.000	5.442E+03	7.800E+05	0.000	1.005E+05
148	NO3 + M ⇔ NO2 + O + M	1.000E+11	0.000	1.800E+05	2.800E+01	1.000	-3.26E+04